Vol 14 No 3, March 2005
1009-1963/2005/14(03)/0599-05

Chinese Physics

© 2005 Chin. Phys. Soc.
and IOP Publishing Ltd

Effect of ion flux on recrystallization and resistance lowering in phosphorus-implanted (0001)-oriented 4H–SiC

Gao Xin(高 欣)[a)†], Sun Guo-Sheng(孙国胜)[a)], Li Jin-Min(李晋闽)[a)],
Zhang Yong-Xin(张永兴)[b)], Wang Lei(王 雷)[a)],
Zhao Wan-Shun(赵万顺)[a)], and Zeng Yi-Ping(曾一平)[a)]

[a)] *Novel Semiconductor Material Laboratory, Institute of Semiconductors, Chinese Academy of Sciences, Beijing* 100083, *China*

[b)] *School of Physical Science and Technology, Lanzhou University, Lanzhou* 730000, *China*

(Received 25 May 2004; revised manuscript received 4 November 2004)

High-dose ion implantation of phosphorus into 4H–SiC (0001) has been investigated with three different ion fluxes ranging from 1.0 to 4.0×10^{12} $P^+cm^{-2}\cdot s^{-1}$ and keeping the implantation dose constant at 2.0×10^{15} P^+cm^{-2}. The implantations are performed at room temperature and subsequently annealed at 1500°C. Photoluminescence and Raman scattering are employed to investigate the implantation-induced damages and the residual defects after annealing. The electrical properties of the implanted layer are evaluated by Hall effect measurements on the sample with a van der Pauw configuration. Based on these results, it is revealed that the damages and defects in implanted layers can be greatly reduced by decreasing the ion flux. Considering room temperature implantation and a relatively low annealing temperature of 1500°C, a reasonably low sheet resistance of 106Ω/□ is obtained at ion flux of 1.0×10^{12} $P^+cm^{-2}\cdot s^{-1}$ with a donor concentration of $4.4\times10^{19}cm^{-3}$.

Keywords: ion implantation, silicon carbide, phosphorus, photoluminescence
PACC: 7460M, 7855, 3220F

1. Introduction

Silicon carbide (SiC) is a promising material for high-power, high-temperature, and high-frequency devices owing to its superior properties such as wide band-gap, high breakdown field, high thermal conductivity, and high saturation electron drift velocity.[1] The selective-area doping technique is one of the indispensable technologies for fabricating planar devices on semiconductors. It is difficult to use the conventional diffusion techniques to produce the heavily doped layers such as the source and drain regions in field effect transistors because the diffusivity of impurities in SiC is negligibly small at temperature below 1800°C.[2] However, ion implantation offers an attractive alternative to the diffusion technique. With ion implantation, one can precisely control the average depth and dose of the dopants by adjusting acceleration voltage and ion current during the implantation, respectively. In order to reduce the resistivity of ohmic contact as well as the source/drain area in field-effect transistors (FETs) such as junction FETs, metal–semiconductor FETs, and metal–oxide–semiconductor FETs,[3] ion implantation with high donor dose into SiC wafers is required.

Nitrogen (N) and phosphorous (P) act as shallow donors in SiC when residing at carbon[4] and silicon[5] lattice sites, respectively. However, implanted N atoms tend to be electrically inactive at an N concentration of more than $2\times10^{19}cm^{-3}$ due to the precipitation and/or the clustering of the dopants formed during postimplantation annealing.[6] Thus P-implantation is superior to N-implantation at higher dose to obtain lower sheet resistance.

At present, SiC-based devices are mainly fabricated in epilayers of 4H- or 6H–SiC with (0001) faces. To activate the doped impurities and to eliminate the implantation damage in the implanted layer, the hot-implantation process is generally employed in the high-dose implantation with subsequent annealing of the implanted layer at high temperatures (HT) around

†E-mail: gaoxin@red.semi.ac.cn

1700°C. However, such extremely high annealing temperature causes some serious problems such as evaporation of the implanted layer, redistribution of the implanted dopants and formation of a macro step structure on the surface. To establish an implantation process similar to Si technology, there exist some major obstacles to be overcome, including successful implantation at room temperature (RT), reduction of annealing temperature, and keeping surface flatness during annealing.

Much work has been devoted to optimize ion implantation parameters, but little work has been done to investigate the ion flux effect in SiC. Only recently, some measurements of implantation damage evolution in ion implanted SiC were reported by Zhang *et al* [7] and Kuznetsov[8] as a function of ion flux. However, in their work no results were reported about the effects of ion flux on the lattice recovery of implantation-induced damages after high temperature annealing and the resultant electrical properties. This paper presents preliminary results on the effects of ion flux on the recrystallization of P-implantation-induced damages in (0001)-oriented 4H–SiC after annealing at 1500°C for 15min and the ensuing electrical properties.

2. Experiment

Samples used are 10-μm-thick, Al-doped (p-type) epitaxial layer, with a doping concentration of 5×10^{16}cm^{-3}, grown on n-type 8° off-axis 4H–SiC (0001) from Cree, Inc. and cut into 5×5 mm^2 pieces for the P ion implantation. Multiple-flux implantations of P^+ (energy: 50–450keV, total dose: 2.0×10^{15}cm^{-2}) were carried out at RT to obtain a 0.5-μm-deep box profile of P. The targets are all tilted 7° from the normal direction during implantation to minimize channelling effects. The mean concentration of P atoms at the plateau of the box profile is 4.4×10^{19}cm^{-3}.The implanting energies and dose ratios were 450, 280, 140, 50keV and 0.38, 0.26, 0.2, 0.16, respectively, based on the results of calculations using the Transport of Ions in Matter (TRIM) simulation program.[9] The ion fluxes for three samples P1, P2 and P3 are 1.0, 2.0 and 4.0×10^{12} P^+cm$^{-2}\cdot$s^{-1}, respectively. Postimplantation annealing was performed in a CVD reactor at 1500° for 15min in pure Ar atmosphere. The implanted layers have been investigated before and after annealing using RT microscopic Raman Scattering and low temperature Photoluminescence (LT PL), which have been verified to be nondestructive and effective methods to investigate the effects of ion implantation and annealing on SiC materials.[10] Raman-scattering experiments were carried out at RT using the 488nm line of Ar ion laser for excitation. The LT PL spectra were measured using a 325-nm He–Cd UV laser and a photon counting system. To measure the electrical properties at RT, Ni electrodes with a van der Pauw configuration were formed on the SiC surface by electron beam evaporation and were then annealed at 1000 °C for 5 min in Ar atmosphere, which results in ohmic contacts. The depth profiles and net doping concentration of the P donors implanted into SiC are measured by secondary-ion mass spectroscopy (SIMS) using a 14.5 keV Cs^+ primary beam. The non-implanted Al-doped epilayer is also measured for comparison.

3. Results and discussion

As an example, Figure 1 shows the phosphorous implantation profiles of the sample P2 annealed at 1500° for 15min. The solid curve is determined with SIMS and the dotted curve is calculated with TRIM simulation program.[9] The overall distribution of P atoms determined by SIMS agrees well with the calculated P profile.

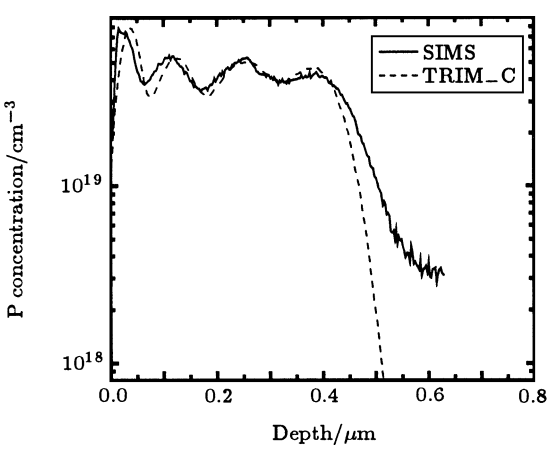


Fig.1. Phosphorus box profile of sample P1 formed by fourfold implantation. The solid curve was determined with SIMS. The dotted curve was calculated with TRIM_C after Ziegler (see Ref.[9]).

Figure 2 shows the LT PL spectra at 10K of the non-implanted sample and the P-implanted ones at different ion fluxes before annealing. It can be clearly seen that the intensities of LT PL spectra in the implanted samples decrease with the increasing ion fluxes. The spectrum features of P1 remain similar to that of the non-implanted one, but the intensity is reduced greatly, while the P3 loses all the 4H–SiC

related features and shows gradual variations of photoluminescence, which is typical of amorphous materials without a clear sharp band edge. The penetration depth in 4H–SiC for 325nm light is about between 7.5μm and 8.4μm.[11,12] For amorphous SiC (a-SiC), light penetration depth is markedly decreased due to the strong optical absorptivities of the amorphous layers. For example, the light penetration depth of a-SiC at 496 nm can be varied between 0.25 and 0.03μm, while the penetration depth for 325nm line should be far less than 0.25μm in a-SiC.[13] No PL emission in P3 was detected, indicating the 325nm exciting light is totally absorbed in the amorphous layer induced by the implantation of higher ion flux. Therefore, the PL spectrum of P1 can come from the single crystalline 4H–SiC beneath the ion-implanted layer and from the partially disordered implanted layer. It can be concluded that lower ion flux can be beneficial to eliminate implantation damages, which is also identical to the observations in Refs.[7,8].

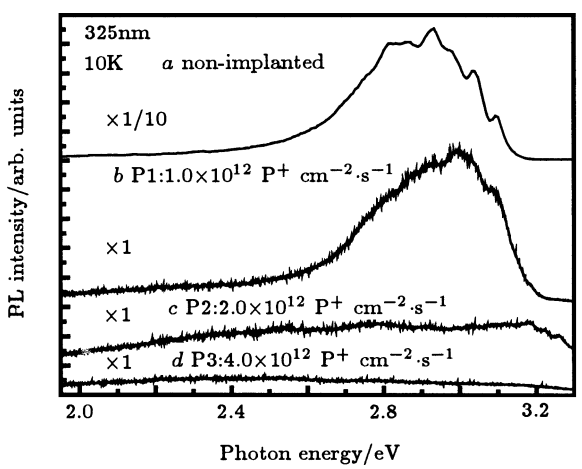


Fig.2. Photoluminescence spectra for 4H–SiC taken at 10K of (a) non-implanted sample, (b) samples P1, (c) P2, and (d) P3 before annealing.

Figure 3 shows the PL spectra at 10K of the implanted samples after annealing at 1500°C for 15 min. After HT annealing, the fundamental 4H–SiC band structure and intensity recovered close to those of the non-implanted sample. It can be observed that the intensity of P1 is higher than those of P2 and P3, while the latter are very close to each other. The lower intensities of P2 and P3 are probably due to a small amount of residual lattice defects, which are not annealed out at HT. The main peaks come from the recombination of the donor-acceptor pair (DAP) and the recombination of a free electron with a hole trapped at an aluminium acceptor. The peak at 3.09eV, designated as A_0, is the zero phonon line of the recombination between free electron and aluminium acceptor.[14] The DAP peaks in the non-implanted sample come from the recombination between the nitrogen donors and aluminium acceptors, while the DAP peaks in the implanted samples are mainly from the recombination between phosphorous donors and aluminium acceptors. This results in a slight difference of DAP peak positions, for the ionization energies of N donors residing at hexagonal and cubic lattice sites are 6–12meV lower than those of P donors.[15] However the A_0 peak positions are the same in both the non-implanted and the implanted ones, and only the peak intensities are different. The A_0 peak intensity of P1 is far higher than those of P2 and P3, indicating that the implanted sample at lower ion flux has more perfect lattice after HT annealing and thus get better recovered. The weaker A_0 peak of the non-implanted sample is due to the lack of free electrons in p-type material, which results in less probability of the recombination between free electron and aluminium acceptor.

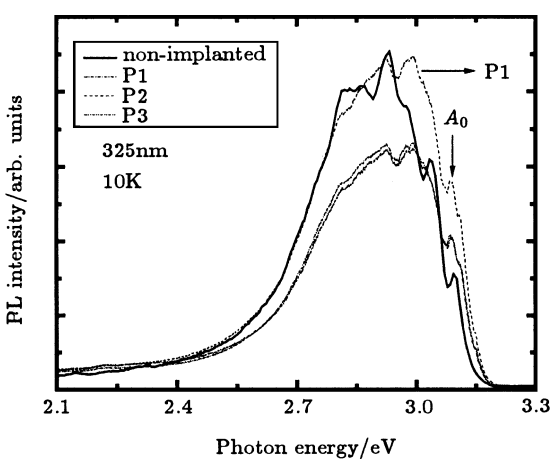


Fig.3. Photoluminescence spectra for 4H–SiC taken at 10K of a non-implanted sample and the ion-implanted samples at various ion fluxes after annealing at 1500° for 15min.

Figure 4 shows Raman scattering spectra of the implanted samples before annealing and the non-implanted one. The Raman spectrum of P3 exhibits totally different spectrum features from that of the non-implanted. No Raman lines of SiC crystallinity are observed and two broad bands appear in the Raman spectrum of the sample P3. The two broad bands correspond to the amorphous atomic vibrations of Si–Si at ~500cm^{-1}, Si–C at ~900cm^{-1},[16] which are typical for amorphous SiC, indicating the damage of 4H–SiC crystallinity and the formation of an amorphous phase. The two broad bands are also observed in the

Raman spectrum of sample P1, but the sharp spectrum lines of 4H–SiC crystallinity are strongly superposed on the top of the Si–C amorphous band. This indicates that the sample P1 implanted at lower ion flux was only partially disordered. The Raman spectrum of P2 is similar to that of P3 and only a quite weak transverse optical (TO) mode at $\sim 777 cm^{-1}$ can be discerned from the broad amorphous bands. After HT annealing, Raman spectra (not shown here) appear close to that of crystalline 4H–SiC with sharp Raman lines of TO modes at ~ 777 and $\sim 796 cm^{-1}$, longitudinal optical (LO) mode at $\sim 964 cm^{-1}$ and longitudinal acoustic (LA) mode at $\sim 204 cm^{-1}$.

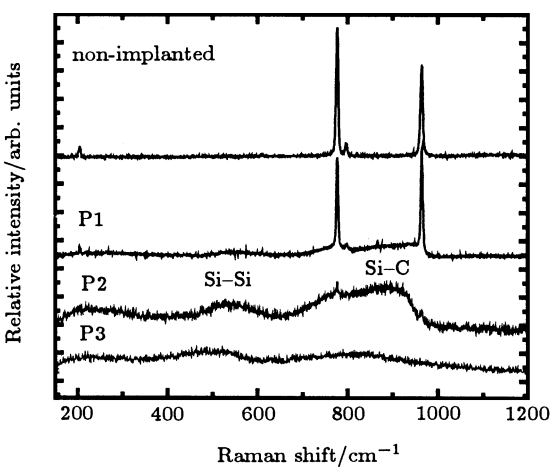


Fig.4. Comparative Raman scattering spectra of the implanted samples before annealing and the non-implanted one.

Figure 5 shows the comparative folded TOs (FTOs) from the non-implanted and the implanted samples annealed at 1500°. For SiC crystals the TO and FTO modes are sensitive to the defects as compared with the LO phonon modes.[17–19] The unfolded TO mode at $796 cm^{-1}$, which is designated as FTO (0), can be used as a monitor band for stacking faults in 6H- and 4H–SiC, which is Raman forbidden at the back scattering geometry using the (0001) face. As can be seen in Fig.5, the FTO (0) intensity of the implanted samples is greatly enhanced relative to that of the non-implanted one and obviously varies with the ion flux. The intensity of P1 is lowest and that of P3 is highest. It can be concluded that after HT annealing the sample implanted at higher ion flux will contain more stacking faults than that implanted at lower ion flux, for a large amount of implantation damage can lead to a recrystallization inducing various polytype crystals[20] during the postimplantation annealing. Furthermore, it can be noted that broadening of the FTO (0) bands is also observed in the annealed samples with the increase of ion fluxes, indicating the increase of stacking disorder with ion flux in the implanted regions after HT annealing.[18]

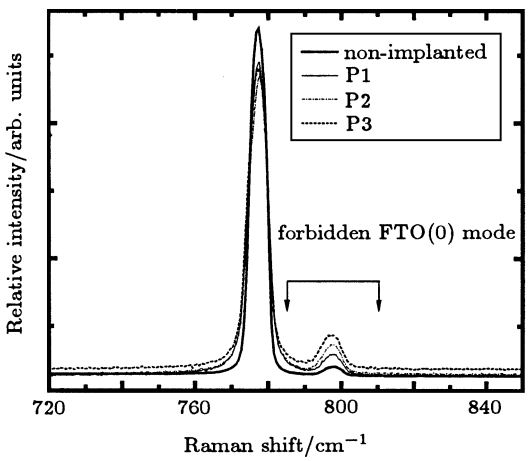


Fig.5. The comparative Raman spectra of FTO (0) bands from the virgin (0001)-oriented 4H–SiC and the ion-implanted samples annealed at 1500°C.

Finally, electrical measurements have been performed. Figure 6 shows the free electron concentration n, sheet resistance R_s, and the Hall mobility μ of the P-implanted samples after HT annealing as a function of ion flux. It can be seen that with the decrease of ion flux the sheet resistivity decreases and both the Hall mobility and the carrier concentration increase. Based on the aforementioned PL and Raman analysis, one can suppose that the difference in carrier concentration and Hall mobility is caused by the residual defects after the HT annealing, because defects can act as trapping centres and can cause the carrier-defect scattering. The sample P1 whose ion flux is lowest has the smallest residual defects after HT annealing, while P3 shows the largest residual defects, but is very close to that of P2, as may be reflected in the small difference of electrical properties between samples P2 and P3. Therefore the lower carrier concentration in samples P2 and P3 can be brought about by the higher compensation introduced by the residual defects.

Nakamura *et al* [21] reported that the phosphorus impurities in the fully amorphized implant-layer substitute the lattice sites more efficiently than in the case of the partially disordered implant-layer in (1–100) or (11–20)-oriented 6H–SiC during annealing process. However, in this case of (0001)-oriented 4H–SiC, the situation is quite the contrary, as can be interpreted by the lack of the atomic stacking sequence of the polytypic structure at the amorphous-crystalline substrate (a/c) interface in the (0001)-oriented 4H–SiC. On the

other hand, in the ion implantation of (1–100) or (11–20)-oriented SiC, the atomic stacking sequence of the polytype is preserved at the (a/c) interface. During the annealing process, the fully amorphized implant-layer in (1–100) or (11–20)-oriented SiC host lattice can be regrown in accordance to the underlying polytype structure and the implanted phosphorus impurities easily occupy the lattice sites without migrating, while in the implantation to (0001)-oriented SiC, the annealing of the amorphous layer can lead to the regrowth of other polytype crystals, which may impede the integration of phosphorus impurities.

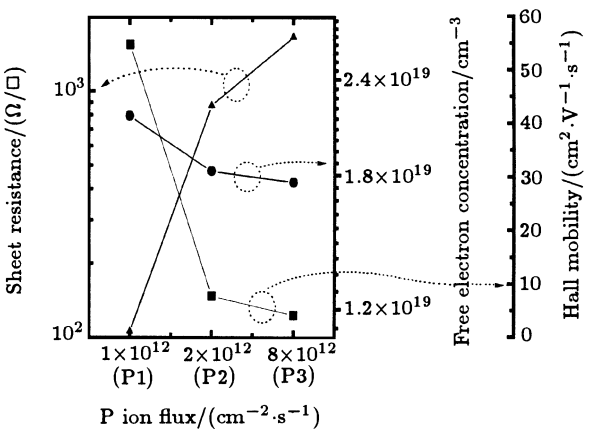


Fig.6. Free electron concentration n, sheet resistivity R_s, and Hall mobility μ of the ion-implanted samples annealed at 1500°C as a function of ion flux.

The resistivity at room temperature ρ_{RT} is equal to $5.3\times10^{-3}\Omega\cdot$cm obtained at the lowest ion flux of 1.0×10^{12} $P^+cm^{-2}\cdot s^{-1}$ for the sample P1, which corresponds to sheet resistance ($R_s=\rho_{RT}/d$) of 106Ω/□, where d=0.5μm is the mean depth of P-implanted layer. Recent studies have shown that a R_s below 100Ω/□ is obtained in the case of 500–800°C implantation into 4H–SiC (0001) and annealing temperatures at 1700°C with donor concentration of about $2.4\times10^{20}cm^{-3}$.[22–24] However, in the present work, RT implantation and lower annealing temperature of 1500°C are used with donor concentration of about $4.4\times10^{19}cm^{-3}$. The use of lower ion flux in ion-implantation may permit the uses of RT implantation and lower annealing temperatures to obtain a reasonably low sheet resistance, when a certain degree of electrically active P donors is demanded.

4. Conclusions

Photoluminescence, Raman scattering and Hall effect measurements have been employed to evaluate the influence of P ion flux on implantation-induced damages and residual defects after HT annealing and the electrical properties. A strong influence of ion implantation flux on the residual defects after HT annealing is observed in 4H–SiC implanted at RT with variation of ion flux from 1.0×10^{12} to 4.0×10^{12} $P^+cm^{-2}\cdot s^{-1}$. It is revealed from the intensities of the A_0 peaks in PL and the appearance of Raman-forbidden FTO (0) bands that lower P ion flux is beneficial to decrease residual defects after HT annealing and thus to reduce the sheet resisitivity with the same implantation dose. A reasonably low R_s of 106Ω/□ was obtained at the lowest ion flux of 1.0×10^{12} $P^+cm^{-2}\cdot s^{-1}$ and annealing at 1500°C for 15 min with a total dose of $2.0\times10^{15}cm^{-2}$. The lower ion flux used in ion-implantation can be an alternative for the uses of RT implantation and lower annealing temperatures for the formation of selective doping areas with lower resistivity on SiC devices.

References

[1] Davis R F *et al* 1991 *Proc. IEEE* **79** 677
[2] Harris G L 1995 *Silicon Carbide* (London: INSPEC) No. 13 Chap. 7
[3] Schmid U *et al* 1999 *J. Appl. Phys.* **85** 2681
[4] Woodbury H H and Ludwig G W 1961 *Phys. Rev.* **124** 1083
[5] Greulich-Weber S *et al* 1995 *Solid State Commun.* **93** 393
[6] Troffer *et al* 1996 *J. Appl. Phys.* **80** 3739
[7] Zhang Y *et al* 2003 *J. Appl. Phys.* **93** 1954
[8] Kuznetsov A Y *et al* 2003 *J. Appl. Phys.* **94** 7112
[9] Ziegler J F and Biersack J P 1985 *The Stopping and Range of Ions in Solids* (New York: Pergamon)
[10] Feng Z C *et al* 1999 *Appl. Phys. Lett.* **75** 472
[11] Sridhara S G *et al* 1999 *Mater. Sci. Eng* B **61–62** 229
[12] Du Y L *et al* 1998 *Acta Phys. Sin.* **47** 1747 (in Chinese)
[13] Derst G *et al* 1989 *Appl. Phys. Lett.* **54** 1722
[14] Ikeda M *et al* 1980 *Phys. Rev.* B **22** 2842
[15] Capano M A *et al* 2000 *J. Appl. Phys.* **87** 8773
[16] Makarov V N *et al* 1994 *Inst. Phys. Conf. Ser.* **137** 545
[17] Nakashima S *et al* 1994 *Phil. Mag.* B **70** 971
[18] Rohmfeld S *et al* 1998 *Phys. Rev.* B **58** 9858
[19] Nakashima S *et al* 2000 *Appl. Phys. Lett.* **77** 3612
[20] Satoh M *et al* 1999 *Nucl. Instrum. Methods Phys. Res.* B **148** 567
[21] Nakamura T *et al* 2003 *Jpn. J. Appl. Phys.* **42** 63
[22] Senzaki J *et al* 2003 *J. Appl. Phys.* **94** 2942
[23] Schmid F *et al* 2002 *J. Appl. Phys.* **91** 9182
[24] Negoro Y *et al* 2002 *Appl. Phys. Lett.* **80** 240